

Structural characterization of a dimeric dimethylindium azide and its use as a single-source precursor for InN thin films

Byoung-Jae Bae, Jae E. Park, Bongsoo Kim, Joon T. Park *

Department of Chemistry and School of Molecular Science (BK21), Korea Advanced Institute of Science and Technology, Taejeon 305-701, South Korea

Received 2 May 2000; received in revised form 17 July 2000; accepted 9 August 2000

Abstract

Dimeric dimethylindium azide, $[\text{Me}_2\text{In}(\mu\text{-N}_3)]_2$ (**1**), was prepared from the reaction of Me_3In with HN_3 . A single-crystal X-ray diffraction study reveals that **1** exists as a three-dimensional network of three symmetry-independent azide-bridged, centrosymmetric dimers. In each dimer, the two azido groups lying in the same plane of the $(\text{In}-\text{N})_2$ ring have a linear geometry, and the two indium atoms exhibit a distorted octahedral geometry. InN thin films were grown with **1** on Si(111) substrates in the temperature range 350–450°C in the absence of carrier gas by a low-pressure chemical vapor deposition method. The stoichiometry of the resulting films was determined by X-ray photoelectron spectroscopy (XPS). The films are nitrogen-deficient InN (In:N \approx 1:0.60) with high surface impurity concentrations (C \approx 20%, O \approx 27%). The film structure was examined by X-ray diffraction (XRD) and scanning electron microscopy (SEM). The films appear to be polycrystalline and show diffraction patterns characteristic of the expected hexagonal wurtzite structure. © 2000 Elsevier Science B.V. All rights reserved.

Keywords: Indium; Azides; Chemical vapour deposition; Indium nitride; Single-source precursors

1. Introduction

The Group 13 nitrides MN (M = Al, Ga, In) and their alloys are currently receiving tremendous attention due to the worldwide demand for high-brightness blue and green light-emitting diodes (LEDs) and laser diodes (LDs) [1]. Recently notable advances have been made for the preparation of thin films of these materials by conventional chemical vapor deposition using mixtures of MR_3 (R = methyl or ethyl) and ammonia (NH_3) [2]. However, high deposition temperatures (> 950°C for AlN and GaN) and high gas-phase ratios ($\text{MR}_3/\text{NH}_3 > 2000$) due to the high thermal stability of NH_3 are general problems in this method, which may lead to unintentional nitrogen vacancies limiting the p-doping capability. Accordingly, the development of single-source precursors as an alternative source has gained increasing attention due to the features of pre-

formed direct M–N bonds and labile leaving groups in the hope of lowering the reaction temperature [3]. Other possible advantages include elimination of the inefficient use of ammonia, minimization of parasitic pre-reactions in the gas phase, and simplification of the processes.

Among the Group 13 nitrides, the growth of InN is most difficult to achieve because of its low decomposition onset, and thus a low-temperature growth is essential for the growth of InN [4]. Recent advances, however, showed that the deposition of InN can be achieved at very low temperature of 300–400°C with the $(\text{N}_3)\text{In}[(\text{CH}_2)_3\text{NMe}_2]_2$ single-source precursor, taking advantage of the unique properties of covalent azides [5]. An azido group is a good candidate for a nitrogen source due to the facile loss of dinitrogen upon thermal or photochemical activation [6]. In this paper we present the synthesis and structural characterization of $[\text{Me}_2\text{In}(\mu\text{-N}_3)]_2$ (**1**) as well as the results of metal–organic chemical vapor deposition (MOCVD) of InN on Si(111) with **1** at low deposition temperatures.

* Corresponding author. Fax: +82-42-869-2810.

E-mail address: jtpark@sorak.kaist.ac.kr (J.T. Park).

2. Experimental

2.1. General comments

All manipulations were carried out by use of standard Schlenk techniques and a Vacuum Atmospheres HE-439 drybox under a dry, oxygen-free argon atmosphere. All solvents were dried according to standard procedures, distilled under argon, and stored over 4 Å molecular sieves prior to use. Trimethylindium was purchased from Strem Chemical Co. and used as supplied. The hydrogen azide (3.1 M solution in ethyl ether) was prepared following literature methods and rigorously dried with anhydrous CaCl_2 [7]. The $^1\text{H-NMR}$ (300 MHz) and $^{13}\text{C-NMR}$ (75 MHz) spectra were recorded on a Bruker AM-300 spectrometer and were referenced to residual protons or carbons of the deuterated solvents. The infrared spectrum (KBr) was obtained with a Bruker Equinox-55 FTIR spectrophotometer. Mass spectral data were collected on a JEOL JMS-SX-102A spectrometer operating in the electron ionization mode. The melting point (uncorrected) was determined using an electrothermal melting point apparatus in a sealed capillary under argon (1 atm). Microanalytical data were provided by the staff of Oneida Research Services, USA.

Table 1
Crystal data and structure refinement for **1**

Formula	$\text{In}_2\text{N}_6\text{C}_4\text{H}_{12}$
Formula weight	373.84
Crystal system	Triclinic
Space group	$P\bar{1}$
Unit cell dimensions	
a (Å)	9.244(5)
b (Å)	10.910(1)
c (Å)	10.920(1)
α (°)	112.44(1)
β (°)	106.39(2)
γ (°)	106.22(2)
V (Å ³)	878.6(5)
Z	3
T (K)	293(2)
D_{calc} (g cm ⁻³)	2.120
Crystal size (mm)	0.65 × 0.30 × 0.20
Radiation	Mo-K α
λ (Å)	0.71069
μ (mm ⁻¹)	3.851
No. of unique reflections	4030
No. of observed reflections ($I > 2\sigma(I)$)	3824 ($R_{\text{int}} = 0.0298$)
Index ranges	$-11 \leq h \leq 11$, $-13 \leq k \leq 12$, $0 \leq l \leq 13$
R^a	0.0406
R_w^b	0.0975
Goodness-of-fit ^c	1.146

$$^a R = (\sum ||F_o| - |F_c||) / \sum |F_o|$$

$$^b R_w = [\sum w(|F_o| - |F_c|)^2] / \sum w|F_o|^2]^{1/2}$$

$$^c \text{Goodness-of-fit} = [\sum w(|F_o| - |F_c|)^2] / (N_{\text{observ}} - N_{\text{params}})]^{1/2}$$

2.2. Synthesis of $[\text{Me}_2\text{In}(\mu\text{-N}_3)]_2$ (**1**)

An ethereal solution of hydrogen azide (3.12 M, 0.815 g, 3.00 mmol) was added dropwise to a stirred toluene solution of Me_3In (0.480 g, 3.01 mmol) at -78°C . The resulting reaction mixture was allowed to warm to room temperature and was stirred for 3 h. Gas evolution (presumably methane) was apparent from the observed frothing. After removal of the solvent and volatiles under reduced pressure, the white residual solid was purified by sublimation (120°C , 10^{-3} Torr) to afford **1** (0.382 g, 1.01 mmol, 68% based on Me_3In) as a colorless solid: m.p. $171\text{--}172^\circ\text{C}$. $^1\text{H-NMR}$ (CDCl_3 , 20°C): δ 0.15 (6H, s, In- CH_3). $^{13}\text{C-NMR}$ (CDCl_3 , 20°C): δ -6.32 (s, In- CH_3). IR (KBr, cm^{-1}): 2056 vs (N_3 , asym), 1350 s (N_3 , sym). MS (EI, 70 eV) m/z 359 ($\text{M}^+ - \text{CH}_3$). Anal. Calc. for $\text{C}_4\text{H}_{12}\text{In}_2\text{N}_6$: C, 12.96; H, 3.21; N, 22.58. Found: C, 12.84; H, 3.23; N, 22.47%.

2.3. X-ray crystallographic study of $[\text{Me}_2\text{In}(\mu\text{-N}_3)]_2$ (**1**)

A crystal suitable for X-ray study was obtained by slow sublimation at 100°C , 10^{-3} Torr. The colorless cubic crystal was mounted in a thin-walled glass capillary under an argon atmosphere, and the capillary was temporarily sealed with silicon grease and then flame sealed. The determination of unit cell parameters and the orientation matrix and the collection of intensity data were made on an Enraf-Nonius CAD-4 diffractometer utilizing graphite-monochromated Mo-K α radiation. The unit cell parameters, occurrences of equivalent reflections, and systematic absences in the diffraction data were consistent with the $P\bar{1}$ space group. Lorentz and polarization corrections were applied to the intensity data while no absorption correction was applied. Intensities of three standard reflections monitored every 4 h showed no significant decay over the course of data collection. Relevant crystallographic details are shown in Table 1. All calculations were performed using the SHELXTL computer programs [8]. Scattering factors for all atoms were included in the software package. The positions of three indium atoms were obtained from a Patterson map and those of the C and N atoms were taken from difference Fourier maps. Full-matrix least-squares refinement based on F^2 was carried out with anisotropic thermal parameters for all non-hydrogen atoms. All hydrogen atoms were placed in calculated positions. In the final cycle of refinement the mean shift/estimated s.d. was less than 0.001.

2.4. Growth of InN thin films

Thin films of InN were grown by a low pressure MOCVD method in a vertical cold-wall reactor on (111) silicon substrates (Fig. 1). Precursor **1** was used as

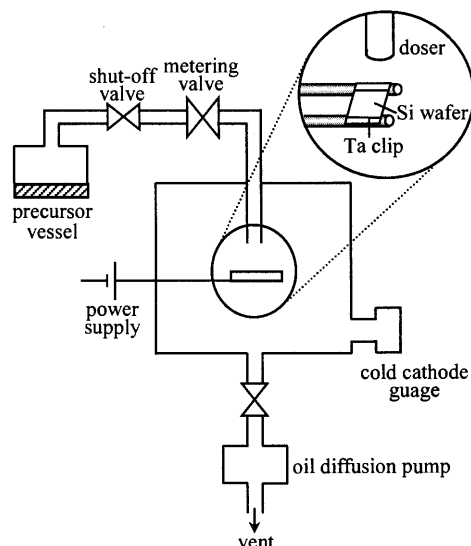


Fig. 1. Schematic diagram of the apparatus used for the growth of InN thin films.

a source material and no carrier gas was used for the deposition. The vacuum chamber was roughed with a mechanical pump and evacuated down to 1.0×10^{-6} Torr by an oil diffusion pump equipped with a liquid nitrogen trap. After the chamber was baked at 150°C for 24 h, the base pressure reached 1.0×10^{-7} Torr. The Si(111) substrate used for the growth was cut into $2.0 \times 1.0 \text{ cm}^2$ samples, rigorously cleaned by a known method [9], and then loaded in the reactor. The substrate temperature was monitored using an optical pyrometer and adjusted to the desired value in the range $300\text{--}1000^\circ\text{C}$. Preheating at 900°C over a 15 min period was provided by passing an electric current through the silicon substrate to liberate any condensed material, and the substrate was brought to the desired deposition temperatures ranging from 350 to 450°C . Precursor was loaded into a stainless steel vessel in a drybox, and introduced into the system through a 1/4 inch stainless steel tube, whose end was approximately 2.0 cm above the surface of substrate. The temperature of the precursor reservoir and the dosing line was then maintained at 100°C throughout the growth to give a reactor pressure of 2.0×10^{-5} Torr. The gas flow rates were controlled by combined metering and shut-off valves and monitored by a cold cathode gauge in the deposition chamber.

When the deposition was finished, the InN films were taken out of the vacuum chamber and stored in an argon atmosphere before the analyses. The obtained films were examined by X-ray diffraction (XRD) measurements using a Rigaku D/MAX-RC 12 kW diffractometer with Cu-K_α radiation. The atomic composition was determined by X-ray photoelectron spectra (XPS) using a VG scientific ESCALAB MK II instrument equipped with Mg-K_α X-ray anode. The

surface morphology, fractured sections and the thickness of the films were checked by scanning electron microscopy (SEM, JEOL JSM 840A). Film adherence was tested by Scotch tape peeling.

3. Results and discussion

3.1. Synthesis and structure of **1**

The azides of Group 13 can be readily prepared by the selective elimination of one equivalent of alkyl chloride from R_3M and ClN_3 . Azido groups can also be introduced by salt metathesis with NaN_3 with the aid of phase-transfer catalysts or THF solvent [10–17]. The dimethylindium azide, $[\text{Me}_2\text{In}(\mu\text{-N}_3)]_2$ (**1**), was prepared from the reaction of Me_3In with HN_3 via methane elimination, and was purified by sublimation under vacuum (120°C , 10^{-3} Torr). Compound **1** is a white solid at room temperature which melts at $171\text{--}172^\circ\text{C}$ without decomposition, and shows poor solubility in non-coordinating, aprotic organic solvents (e.g. toluene, *n*-hexane, dichloromethane). However it dissolves readily in THF or in toluene in the presence of *tert*-butylamine. This observation can be accounted for by the formation of a THF adduct or a *tert*-butylamine adduct of dimethylindium azide. Similar types of Lewis-base stabilized adducts were previously reported in cases of $\text{Me}_2(\text{N}_3)\text{Al}:\text{NH}_2\text{Me}$ [10] or THF adducts of Et_2AlN_3 [11], $\text{Ga}(\text{N}_3)_3$ [12], and Cl_2InN_3 [13]. The dimeric formulation has been indicated by the observation of $[\text{dimer} - \text{Me}]^+$ ion with 100% relative intensity at m/z 359. But a signal for the $[\text{trimer} - \text{Me}]^+$ ion also appears with 0.88% relative intensity at m/z 546 presumably due to the gas-phase oligomerization. This coexistence of dimeric and trimeric species in the gas phase was also observed in the case of $[\text{Me}_2\text{Ga}(\mu\text{-NHNMe}_2)]_2$ [14]. The presence of azide moieties is evident on the basis of the symmetric (1350 cm^{-1}) and asymmetric (2056 cm^{-1}) stretches of the azide moiety in the IR spectrum. Azides of any type should be treated as potentially explosive materials, but **1** showed no explosive nature upon abrupt heating, sharp mechanical impact, contact with air and moisture, sublimation under reduced pressure, or under MOCVD conditions.

In previous work by Rödder and Dehnicke, dimethylindium azide was prepared by the reaction of Me_3In with Me_3SnN_3 and a trimeric formulation, $[\text{Me}_2\text{In}(\mu\text{-N}_3)]_3$, was proposed based on the mass spectroscopic data [15]. In the present work, however, X-ray crystallographic study reveals that compound **1** comprises a three-dimensional network of dimeric units in the solid state as shown in Fig. 2. Three dimeric molecules constitute one unit cell, and each dimer has a crystallographic centrosymmetric structure with a pair

of dimethylindium units bridged by two $\mu\text{-N}_3$ groups. The dimeric units are connected to each other by an extended dative bonding network, involving the indium and terminal nitrogen atom of the azide group of a neighboring molecule, resulting in the formation of a

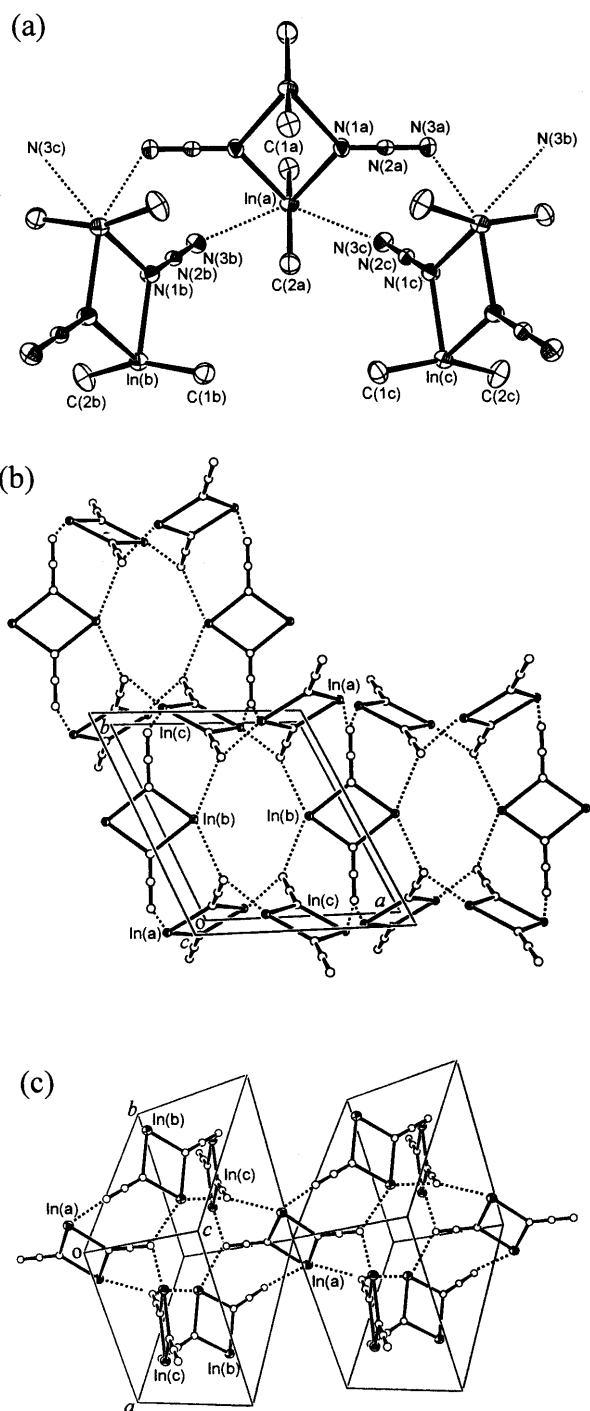


Fig. 2. (a) Molecular structure and atomic labeling scheme of the three symmetry-independent $[\text{Me}_2\text{In}(\mu\text{-N}_3)]_2$ (**1**) molecules with 30% probability thermal ellipsoids. The intermolecular contacts are shown by dashed lines; (b) Perspective view of the unit-cell contents for **1**. In–CH₃ bonds are not drawn for clarity; (c) View of two unit cells aligned in the [111] direction.

three-dimensional framework. As a consequence, the geometry at the hexa-coordinated indium center can be described as distorted octahedral with the coordination of four nitrogen atoms and two carbon atoms as shown in Fig. 2a. Fig. 2b,c show the molecular packing of **1** in the crystal lattice. The chains of dimeric units extend along the *a* axis (bac bac...), *b* axis (abc abc...) and [111] direction (acb acb...). The intermolecular In...N₃ distances (average 2.924(4) Å) are listed in Table 2. Analogous interactions were found previously in the case of $[(\text{N}_3)(\text{NMe}_2)\text{Ga}(\mu\text{-NMe}_2)]_2$ (3.431 Å) [16].

The covalent bonding between the indium and *ipso* nitrogen of bridging azide groups in the same dimer has a length of 2.395(4) Å, which is somewhat longer than the values found in $[\text{Me}_2\text{In}(\mu\text{-N=CMe}_2)]_2$ (2.195(4) Å) [18]. The internal angles in the planar (In–N)₂ core are 73.8(2)° at indium and 106.2(2)° at nitrogen. The obtuse In–N–In' angle and long In...In' separation of 3.829(2) Å indicate that there is no indium–indium bonding interaction. As expected, two different N–N distances are found in the azide unit (1.184(6) and 1.156(6) Å). The shorter N–N distance corresponds to the terminal N₂ moiety, indicating an activated azide towards N₂ elimination. The small difference between alternating N–N distances (0.028 Å) as compared to those of aluminum and gallium azide compounds (0.039–0.138 Å) can be explained by the more ionic nature of the In–N_{azide} bonds [5c]. Selected bond distances and angles of the three equivalent molecules are listed in Table 2.

3.2. Film deposition studies

Synthesis of dialkyl aluminum and gallium azide, $[\text{R}_2\text{M}(\mu\text{-N}_3)]_n$ (R = Me, Et; M = Al, Ga; *n* = 2, 3, ∞), and deposition of MN with these single source precursors are well documented [3,11,15,19]. However the deposition of InN with a homologous dimethylindium azide has not been investigated.

The film growth was achieved on p-type Si(111) substrates without any carrier gas under low pressure MOCVD conditions. A cold-wall reactor was used in the temperature range 350–450°C. Typical run times were 20 h resulting in films with a thickness of 0.5 μm and all films adhered well to substrates. In previous work by Bu and coworkers, no InN film was formed on Si(100) without laser irradiation with separate sources of Me₃In and HN₃ [20]. In contrast, the InN film is formed on the Si(111) surface by thermal pyrolysis without laser assistance in the present work. This observation can be accounted for by the decreased surface reaction energy because of the preformed In–N bonds in the single-source precursor.

Examination by SEM showed a smooth and crack-free morphology for InN film deposited on Si(111) at 350°C as shown in Fig. 3 and no indium droplets were formed at the surface.

Table 2

Bond distances (Å) and angles (°) with estimated S.D. values for three equivalent molecules of $[\text{Me}_2\text{In}(\mu\text{-N}_3)]_2$ (**1**)^a

In–C(1)	2.111(6), 2.111(6), 2.106(6)	In–C(2)	2.120(6), 2.108(6), 2.102(6)
In–N(1)	2.395(4), 2.390(4), 2.393(4)	In–N(1')	2.397(4), 2.398(4), 2.395(4)
N(1)–N(2)	1.185(6), 1.187(6), 1.179(6)	N(2)–N(3)	1.151(6), 1.157(6), 1.159(6)
In⋯In'	3.833(2), 3.828(2), 3.825(2)	In(a)⋯N(3b)	2.920(5)
In(a)⋯N(3c)	2.924(5)	In(b)⋯N(3a)	2.921(5)
In(b)⋯N(3c')	2.934(5)	In(c)⋯N(3a')	2.927(5)
In(c)⋯N(3b')	2.929(5)		
C(1)–In–C(2)	158.6(3), 158.1(3), 158.4(3)	C(1)–In–N(1)	98.4(2), 98.2(2), 98.2(2)
C(2)–In–N(1)	98.8(2), 99.5(3), 99.1(3)	N(1)–In–N(1')	73.8(2), 73.8(2), 73.9(2)
In–N(1)–In'	106.2(2), 106.2(2), 106.1(2)	In–N(1)–N(2)	126.7(3), 126.7(3), 126.6(3)
N(1)–N(2)–N(3)	179.6(5), 179.5(5), 179.5(5)		

^a Three symmetry-independent units are labeled with a, b, and c and atoms related by the *i*-symmetry operations are labeled with a prime.

X-ray diffraction studies reveal that a hexagonal wurtzite phase of InN is grown with the preferred orientation of the (0002) direction (Fig. 4). Although the film deposited is polycrystalline, it shows better crystallinity than that deposited with $(\text{N}_3)\text{In}[(\text{CH}_2)_3\text{NMe}_2]_2$, which is the only single-source precursor reported for InN thin film [5]. The calculated lattice parameters ($a = 3.596$ and $c = 5.711$ Å) agree well with those of bulk indium nitride ($a = 3.533(4)$ and $c = 5.693(4)$ Å) prepared from $(\text{NH}_4)_3\text{InF}_6$ at 600°C [21]. For the films deposited at 400–450°C, the conversion of diffracted intensity from linear to logarithmic scale reveals the diffraction peaks due to elemental indium, indicating nitrogen-deficient films (Fig. 4b). However, a drop of the deposition temperature to 350°C led to the disappearance of these diffraction peaks (Fig. 4a). No diffraction peak from cubic indium oxide is observed at the temperature range 350–450°C.

The stoichiometric nature of the films was examined by X-ray photoelectron spectroscopy. The deposited film is identified as InN by the presence of In(3d_{5/2}) and N(2s) XPS peaks at 443.4 and 397.0 eV, respectively. For film deposited at 350°C, the ratio of indium to nitrogen is 1:0.6 at the surface. Sputtering ca. 100 Å of the film with an Ar beam led to preferential elimination of nitrogen, thus it was difficult to establish In/N stoichiometry exactly. Cowley et al., who have studied GaN films grown with $[\text{Me}_2\text{Ga}(\mu\text{-N}_3)]_n$ [14a,19e], have also observed similar results. The measured C and O impurity levels at the surface are 21 and 27%, decreasing to 11 and 8%, respectively, upon sputtering ca. 100 Å of the film. The remaining high carbon content may have stemmed from incomplete decomposition of In–C(methyl) bonds, presumably because a high reaction energy is required for the homolytic cleavage of this bond [3d,13a]. The low vapor pressure of precursor **1** results in low growth rates of films (0.025 μm h⁻¹), which causes residual water and oxygen in vacuo to incorporate into the growing InN film as oxides.

In summary, InN films have been deposited on Si substrates at low pressure and temperatures using

$[\text{Me}_2\text{In}(\mu\text{-N}_3)]_2$ (**1**) which consists of a three-dimensional network of dimers in the solid state. The crystalline quality of InN films grown from **1** is superior to that of films obtained with $(\text{N}_3)\text{In}[(\text{CH}_2)_3\text{NMe}_2]_2$ single-source precursor [5].

4. Supplementary material

Crystallographic data for the structural analysis have been deposited with the Cambridge Crystallographic Data Centre, CCDC no. 130244 for compound **1**. Copies of the data can be obtained free of charge on application to The Director, CCDC, 12 Union Road, Cambridge CB2 1EZ, UK (Fax: +44-1223-336033; e-mail: deposit@ccdc.cam.ac.uk or www: http://www.ccdc.cam.ac.uk).

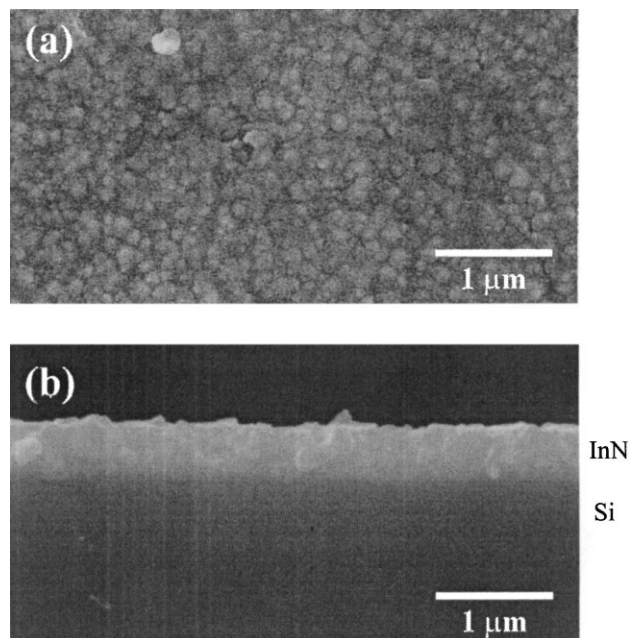


Fig. 3. (a) SEM image taken from InN film grown at 350°C; (b) a cross-sectional view of InN film 0.5 μm thick on a cleaved Si substrate.

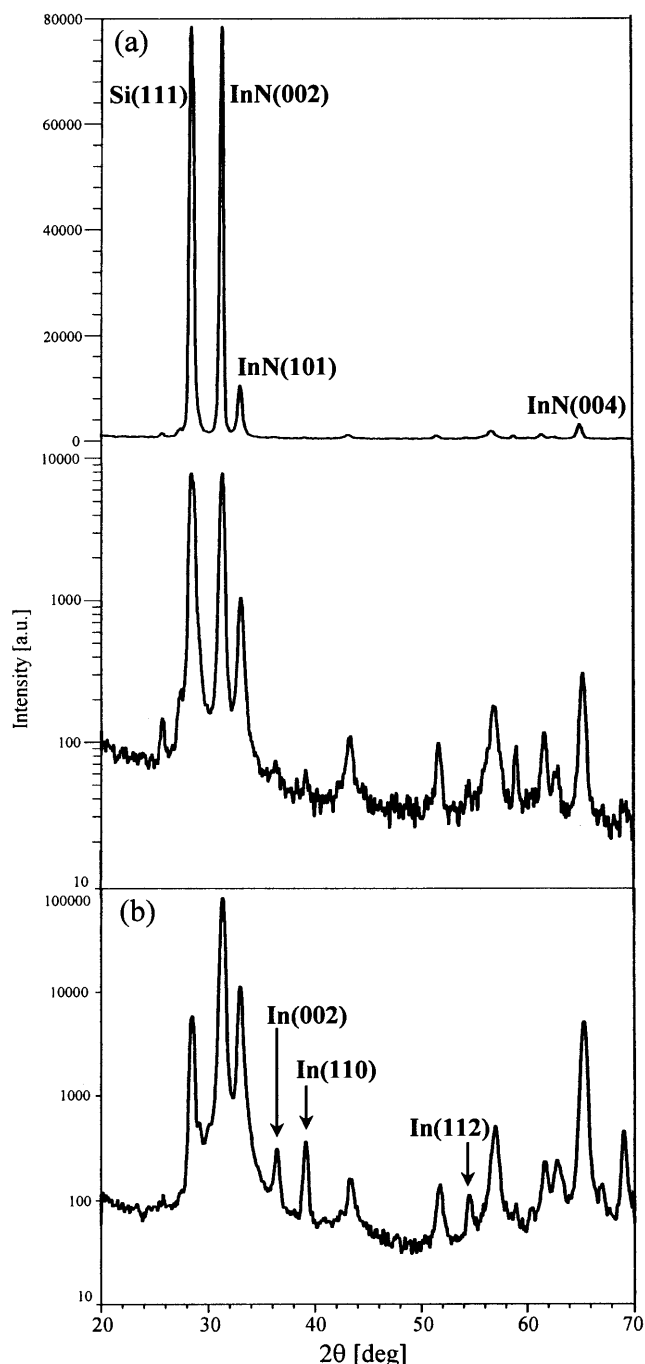


Fig. 4. (a) X-ray diffraction patterns of InN grown at 350°C on Si(111) without a carrier gas; (b) formation of metallic indium at 450°C.

Acknowledgements

This work was supported by the Brain Korea 21 Project.

References

- [1] (a) S. Nakamura, G. Fasol, *The Blue Laser Diode*, Springer, Berlin, 1997. (b) S. Strite, H. Morkoç, *J. Vac. Sci. Technol. B* 10 (1992) 1237. (c) H. Morkoç, S. Strite, G.G. Gao, M.E. Lin, B. Sverdlov, M. Burns, *J. Appl. Phys.* 76 (1994) 1363. (d) H. Morkoç, S.N. Mohammad, *Science* 267 (1995) 51.
- [2] (a) H. Amano, N. Sawaki, I. Akasaki, Y. Toyoda, *Appl. Phys. Lett.* 48 (1986) 353. (b) S. Nakamura, *Jpn. J. Appl. Phys.* 30 (1991) L1705. (c) S. Nakamura, *Appl. Phys. Lett.* 58 (1991) 2021. (d) M.A. Khan, J.N. Kuznia, D.T. Olson, R. Kaplan, *J. Appl. Phys.* 73 (1993) 3108. (e) A. Saxier, P. Kung, C.J. Sun, E. Bigan, M. Razeighi, *Appl. Phys. Lett.* 64 (1994) 339.
- [3] (a) A.C. Jones, P. O'Brien, *CVD of Compound Semiconductors*, VCH, Weinheim, 1997, Chapter 3. (b) A.C. Jones, C.R. Whitehouse, J.S. Roberts, *Chem. Vap. Deposition* 1 (1995) 65. (c) T.D. Getman, G.W. Franklin, *Comments Inorg. Chem.* 17 (1995) 79. (d) D.A. Neumayer, J.G. Ekerdt, *Chem. Mater.* 8 (1996) 9.
- [4] (a) J.B. MacChesney, P.M. Bridenbaugh, P.B. O'Connor, *Mater. Res. Bull.* 5 (1970) 738. (b) Q. Guo, O. Kato, A. Yoshida, *J. Appl. Phys.* 1 (1993) 7969.
- [5] (a) R.A. Fischer, A. Miehr, T. Metzger, E. Born, O. Ambacher, H. Angerer, R. Dimitrov, *Chem. Mater.* 8 (1996) 1356. (b) R.A. Fischer, A. Miehr, O. Ambacher, T. Metzger, E. Born, *J. Cryst. Growth* 170 (1997) 139. (c) R.A. Fischer, H. Sussek, A. Miehr, H. Pritzkow, E. Herdtweck, *J. Organomet. Chem.* 548 (1997) 73. (d) R.A. Fischer, H. Sussek, H. Parala, H. Pritzkow *J. Organomet. Chem.* 592 (1999) 205.
- [6] (a) H. Beck, R. Dammel, *Angew. Chem. Int. Ed. Engl.* 26 (1987), 504. (b) Z. Dori, R.F. Ziolo, *Chem. Rev.* 73 (1973) 247. (c) H. Beck, R. Dammel, *J. Am. Chem. Soc.* 110 (1988) 5261. (d) C. Guimon, G. Pfister-Guillouzo, *Organometallics* 6 (1987) 1387. (e) J. Chatt, C.D. Falk, G.J. Leigh, R.J. Paske, *J. Chem. Soc. A* (1969) 2288.
- [7] L.F. Audrieth, C.F. Gibbs, *Inorg. Synth.* 1 (1939) 77.
- [8] (a) G.M. Sheldrick, *SHELXS86*, *Acta Crystallogr. Sect. A* 46 (1990) 467. (b) G.M. Sheldrick, *SHELXL93*, Program for the Refinement of Crystal Structures, University of Göttingen, Germany, 1993.
- [9] A. Ishizaka, Y. Shiraki, *J. Electrochem. Soc.* 133 (1986) 666.
- [10] R.A. Fischer, A. Miehr, H. Sussek, H. Pritzkow, E. Herdtweck, J. Müller, O. Ambacher, T. Metzger, *Chem. Commun.* (1996) 2685.
- [11] M.I. Prince, K. Weiss, *J. Organomet. Chem.* 5 (1966) 594.
- [12] R.A. Fischer, A. Miehr, E. Herdtweck, M.R. Mattner, O. Ambacher, T. Metzger, E. Born, S. Weinkauff, C.R. Pulham, S. Parsons, *Chem. Eur. J.* 2 (1996) 1353.
- [13] C. Steffek, J. McMurrin, B. Pleune, J. Kouvetakis, T.E. Concolino, A.L. Rheingold, *Inorg. Chem.* 39 (2000) 1615.
- [14] (a) V. Lakhotia, D.A. Neumayer, A.H. Cowley, R.A. Jones, J.G. Ekerdt, *Chem. Mater.* 7 (1995) 546. (b) D.A. Neumayer, A.H. Cowley, A. Decken, R.A. Jones, V. Lakhotia, J.G. Ekerdt, *Inorg. Chem.* 34 (1995) 4698. (c) K. Kim, J.H. Kim, J.E. Park, H. Song, J.T. Park, *J. Organomet. Chem.* 545–546 (1997) 99.
- [15] N. Rödder, K. Dehnicke, *Chimia* 28 (1974) 349.
- [16] D.A. Neumayer, A.H. Cowley, A. Decken, R.A. Jones, V. Lakhotia, J.G. Ekerdt, *J. Am. Chem. Soc.* 117 (1995) 5893.
- [17] (a) A. Miehr, O. Ambacher, W. Rieger, T. Metzger, E. Born, R.A. Fischer, *Chem. Vap. Deposition* 2 (1996) 51. (b) A.C. Frank, F. Stowasser, H. Sussek, H. Pritzkow, C.R. Miskys, O. Ambacher, M. Giersig, R.A. Fischer, *J. Am. Chem. Soc.* 120 (1998) 3512. (c) S. Schulz, M. Nieger, *J. Chem. Soc., Dalton Trans.* (1998) 4127. (d) J. Müller, R.A. Fischer, H. Sussek, P. Pilgram, R. Wang, H. Pritzkow, E. Herdtweck, *Organometallics* 17 (1998) 161.
- [18] F. Weller, U. Müller, *Chem. Ber.* 112 (1979) 2039.

- [19] (a) J. Müller, K. Dehnicke, *J. Organomet. Chem.* 12 (1968) 37. (b) V.V. Krieg, J. Weidlein, *Z. Anorg. Allg. Chem.* 368 (1969) 44. (c) D.C. Boyd, R.T. Haasch, D.R. Mantell, R.K. Schulze, J.F. Evans, W.L. Gladfelter, *Chem. Mater.* 1 (1989) 119. (d) J. Kouvetakis, D.B. Beach, *Chem. Mater.* 1 (1989) 476. (e) D.A. Atwood, R.A. Jones, A.H. Cowley, J.L. Atwood, S.G. Bott, *J. Organomet. Chem.* 394 (1990) C6. (f) C.J. Carmalt, A.H. Cowley, R.D. Culp, R.A. Jones, *Chem. Commun.* (1996) 1453.
- [20] (a) Y. Bu, M.C. Lin, *Mater. Res. Soc. Symp. Proc.* 335 (1994) 21. (b) Y. Bu, L. Ma, M.C. Lin, *J. Vac. Sci. Technol. A* 11 (1993) 2931.
- [21] V.R. Juza, H. Hahn, *Z. Anorg. Allg. Chem.* 239 (1938) 282.